Reptation Time, Temperature, and Cosurfactant Effects on the Molecular Interdiffusion Rate during Polystyrene Latex Film Formation

Kyung Don Kim,[†,‡,§,¶] **L. H. Sperling,***[,†,‡,§,∥,¶] **and A. Klein**[†,§,⊥,¶]

Center for Polymer Science and Engineering, Materials Research Center, Department of Chemical Engineering, Department of Materials Science and Engineering, Emulsion Polymer Institute, and Polymer Interfaces Center, Whitaker Laboratory No. 5, Lehigh University, Bethlehem, Pennsylvania 18015

B. Hammouda

Materials Science and Engineering Laboratory, National Institute of Standards and Technology, Building 235, E 151, Gaithersburg, Maryland 20899

Received August 23, 1993; Revised Manuscript Received August 4, 1994[⊛]

ABSTRACT: The interdiffusion of polymer chains during film formation from direct mini-emulsified deuterated and protonated polystyrenes (DPS = mol wt 150 000 and 185 000; HPS = mol wt 150 000 and 200 000) was characterized by small-angle neutron scattering (SANS) and tensile strength measurements. Films containing 6 mol % deuterated particles were annealed at several temperatures above T_g for various periods of time. The average interpenetration depth of deuterated polystyrene chains depended on the one-fourth power of the annealing time up to the reptation time, τ, shifting to the one-half power after the reptation time. The center of mass diffusion coefficients from the SANS data were 2.4×10^{-16} cm^2/s for M_n = 150 000 and 1.5×10^{-16} cm^2/s for M_n = 185 000 at an annealing temperature of 135 °C. The diffusion activation energies of the present system were 52 ± 4 kcal/mol for the temperature range $125 \leq T \leq 155$ °C. Full tensile strength was achieved at a penetration depth of 90–100 Å, which is comparable to 0.81 times the radius of gyration of the whole polystyrene chain (86 Å for M_n = 150 000) predicted theoretically. Finally, latex samples containing 1.5 wt % cosurfactants showed a faster interdiffusion rate especially at $t > \tau$ and a smaller activation energy than the corresponding pure latex sample.

Introduction

The use of latex films to investigate molecular interdiffusion is important both in theory and in applications such as coating, adhesion, welding, and crack healing. Difficulties in interpreting data based on broad particle sizes and molecular weights have been encountered in studying the final process of latex film formation, namely interdiffusion of polymer chains between latex particles to make continuous films.

There are two basic methods of studying the diffusion of polymer molecules across the boundary between particles in a latex system, small-angle neutron scattering (SANS) via measurement of latex blends of deuterated and protonated latex particles[1-6] and a fluorescence technique.[7-12]

The advantages of SANS lie in its high sensitivity and the ability to determine the diffusion coefficient and chain interpenetration depth easily. As the first researchers in this area, Hahn et al.[1,2] used *n*-butyl methacrylate copolymer and Linne et al.[3] used polystyrene to study chain interdiffusion of broad molecular weight distribution polymers via SANS. They found an increase in the radius of gyration of polymer chains during the course of film annealing, which provided evidence of interdiffusion between latex particles. Anderson and Jou[4] prepared deuterated and protonated polystyrene latex particles having narrow molecular weight distributions by direct emulsification. Using a 68 000 molecular weight sample at 130 °C, they obtained diffusion coefficients of 1.8×10^{-15} cm^2/s for polystyrene during the annealing of latex films via SANS.

Yoo et al.,[5,6] also using polystyrene and the SANS technique, worked out the relationship between the increase in mechanical strength and the interdiffusion depth during film formation. Their results were consistent with Wool's crack-healing theory[13,14] based on de Gennes' reptation model.[15] However, the effects of molecular weight distribution and chain end groups on chain diffusion were not determined and still remain as unsolved problems.

More recently,[16,17] artificial latexes having both a narrow molecular weight distribution and good particle size uniformity were prepared by a new direct mini-emulsification technique. This system had a higher interdiffusion rate and a higher tensile strength than the emulsion-polymerized latex system at similar annealing times. The differences between the present results and Yoo et al.'s may be due to the broad molecular weight distribution of their samples and/or to different chain end groups.

The other interesting method utilizes fluorescence, which has been mainly applied to latex film formation by Winnik and co-workers.[7-12] In this technique, latexes are prepared in two different batches. In one batch, the chains contain a "donor" group, while in the other, an "acceptor" group is attached. Polymer diffusion was studied by direct nonradiative energy transfer (DET) measurement. By the evaluation of the diffusion coefficients of poly(*n*-butyl methacrylate) (PBMA) and poly(methyl methacrylate) (PMMA) latex systems, they studied the interdiffusion of polymer chains between neighboring latex particles.

Some recent studies[5,6,17] have confirmed that polymer chain interdiffusion between latex particles is consistent with Wool's minor chain reptation theory[13,14] of polymer interface healing. It is based on de Gennes' reptation

† Center for Polymer Science and Engineering.
‡ Materials Research Center.
§ Department of Chemical Engineering.
∥ Department of Materials Science and Engineering.
⊥ Emulsion Polymer Institute.
¶ Polymer Interfaces Center.
⊛ Abstract published in *Advance ACS Abstracts*, September 15, 1994.

0024-9297/94/2227-6841$04.50/0

model[15] at annealing times longer than the reptation time. The reptation time, τ, was defined by de Gennes, as the time required by the molecule to diffuse a distance equal to its radius of gyration R_g, as $\tau = 2R_g^2/\pi^2 D$, where D is the self-diffusion coefficient. However the dynamics of polymer chains up to the reptation time during latex film formation is not well understood. According to the reptation model, the diffusion process is dominated by the segmental motion at times shorter than the reptation time, while the center of mass diffusion prevails at times longer than the reptation time. As pointed out by Wool in his recent papers,[13,14,18-20] time dependent chain properties in bulk polymers show totally different reptation time scaling laws.

Some studies on the temperature dependence of the self-diffusion coefficient have been carried out in the bulk state.[20-24] The activation energy from diffusion data in the bulk state compared well with values obtained from viscoelastic measurements. Winnik et al.[7,8,10-12] calculated diffusion coefficients for various diffusion temperatures in latex systems and found them to be consistent with the WLF equation.

The other important point is the effect of the surfactant and co-surfactant on the diffusion rate and the properties of the film. Voyutskii[25] reported earlier that surfactants could remain in the film as an independent structural network or be dissolved in the polymer. In the first case, the presence of surfactants increases the heterogeneity of the film. However, in the second case, the surfactants can increase the autoadhesion and formation rates of film formation.

Zhao et al.[26] have analyzed the distribution of a surfactant in latex film via Fourier transform infrared-attenuated total reflection (FTIR-ATR) and investigated the effect of the surfactant on the adhesion properties of coalescent latex films. A similar study on surfactant dispersion at the latex film interfaces has been carried out by Urban et al.[27] Both researchers found that the surface activity of surfactants and the surfactants compatibility with the polymer affected the surfactant dispersion, which determined the properties of films.

These studies show that latex film formation rates and the properties of films can be altered by a small amount of surfactant. Wang and Winnik[9,11] have seen that the polymer diffusion rate rapidly increases with the addition of a film-forming additive. They regarded this result as a plasticizer effect to increase the free volume in the film.

The present direct mini-emulsification technique uses two long chain alcohols as cosurfactants, that is, cetyl alcohol, $CH_3(CH_2)_{15}OH$, and stearyl alcohol, $CH_3(CH_2)_{17}OH$. These long chain alcohols have a high miscibility with polystyrene. In a previous study,[17] co-surfactants were completely removed to investigate pure polymer chain interdiffusion at the particle–particle interfaces. However, in practical applications, the presence of cosurfactants during film formation is inevitable.

In this paper, the polymer diffusion process during the course of annealing was studied by SANS. An improved direct mini-emulsification technique was used to prepare artificial latexes.[16] Films were annealed at several different temperatures and times to observe the chain behavior around the reptation (disengagement) time and temperature dependence of the interdiffusion process. Finally, polystyrene containing 1.5 wt % cetyl alcohol and stearyl alcohol was investigated by SANS. SANS data were correlated with tensile strength values, and the activation energy was obtained by Arrhenius plots. The results were compared with published data on polymer diffusion at interfaces[17,20,22-24] and interpreted using quantitative models.[21,28]

Theoretical Background

SANS Data Analysis. The average interpenetration depth of polymer chains during the course of film formation was determined from the apparent expansion of the radius of gyration, R_g, of the deuterated polystyrene latex particles. The quantity R_g was calculated from the well-known Guinier approximation[29] in the low-angle region as

$$\frac{d\Sigma}{d\Omega}(Q) = \frac{d\Sigma}{d\Omega}(0)\exp(-Q^2R_g^2/3) \quad (1)$$

where $d\Sigma/d\Omega$ represents the coherent scattering cross section per unit volume of the material and Q is the scattering wave vector. The value for R_g can be obtained from the slope of the plot of logarithmic intensity vs Q^2. A sphere of radius R is related to the radius of gyration by

$$R^2 = (5/3)R_g^2 \quad (2)$$

The time dependent average interpenetration depth, $d(t)$, of the polymer chains across the particle boundaries was obtained by subtracting the radius, R, of the deuterated latex particles in the dispersed state from the radius, $R(t)$, of the expanding deuterated polystyrene particles as

$$d(t) = R(t) - R \quad (3)$$

where t represents the annealing time.

For a system composed of randomly mixed clusters of protonated and deuterated polymers, Summerfield and Ullman[30,31] derived an equation for the time dependent scattering intensity based on Fick's law. They showed that $I(Q,t)$, the SANS intensity after annealing for time t, can be expressed as

$$I(Q,t) = I(Q,0)\exp(-2DQ^2t) + a(t)I(Q,\infty) \quad (4)$$

where $I(Q,0)$ and $I(Q,\infty)$ are the initial and equilibrium scattering intensities, respectively, and D is the diffusion coefficient. The factor $a(t) = 1 - \alpha(0,t)$, where $\alpha(0,t)$ is the normalized integral of radial correlation function, $\gamma(R,0)$, characterizing the initial segregation in the unannealed sample at time $t = 0$, and can be expressed as

$$\alpha(0,t) = (8\pi Dt)^{-3/2}\int_0^\infty \gamma(R,0)\exp(-R^2/8Dt)\,dR \quad (5)$$

where R is a radial position. By definition, $\alpha(0,\infty) = 0$ and $a(\infty) = 1$ for homogeneous samples at infinite annealing time.

The present SANS data show that $I(Q,\infty)$ is much smaller (less than a factor of 10) than $I(Q,0)$ at low angles and short annealing times, which results in neglect of the second term of eq 4 with little error. $I(Q,\infty)$ is from fully annealed samples and represents the scattering from the blend.

For a partly annealed sample, the experimental diffusion coefficients can be calculated by combining data at a certain range of Q values and annealing times. In order to characterize Q and time dependent effects, the Q-constant diffusion coefficient, D_Q, and the time-constant diffusion coefficient, D_t, were calculated by

$$D_Q = -\frac{1}{2}\{d[\ln[I(Q,t)/I(Q,0)]]/dt\}_Q/Q^2 \quad (6)$$

$$D_t = -\frac{1}{2}\{d[\ln[I(Q,t)/I(Q,0)]]/dQ^2\}_t/t \quad (7)$$

respectively. The present SANS data were obtained in the range $0.003 \le Q \le 0.034$ Å^{-1}, but analyzed in the range $0.003 \le Q \le 0.01$ Å^{-1} to calculate diffusion coefficients.

Average Chain Interpenetration Depth, $d(t)$. The model for the motion of individual chains in amorphous bulk materials has been established by the reptation theory of de Gennes[15,32] and Doi and Edwards.[33] In this model the molecules move in a curvilinear fashion along their own contours constrained by their neighboring molecules. The constrained region is often referred to as a tube in which the molecule can slither or reptate back and forth. On the basis of this theory Kim and Wool[14] developed the minor chain reptation model to describe the motion of the minor chains at the interface and calculated the average interpenetration depth of polymer segments as a function of time. According to their model, the chain ends of the molecule diffuse with time, and part of the molecule, the minor chain, escapes from the original constrained space or tube. Eventually, the whole chain escapes from its initial conformation at the diffusion time $t = \tau$. At $t > \tau$, the chain diffusion is regarded primarily as a center of mass motion. Of course, new tube conformations are continuously selected in a random fashion.

Depending on the reptation time, the average chain interpenetration depth, $d(t)$, was found to scale as follows[14,15]

$$d(t) \propto t^{1/4}M^{-1/4} \quad t < \tau \quad (8)$$

$$d(t) \propto t^{1/2}M^{-1} \quad t > \tau \quad (9)$$

where M is the molecular weight. At $t = \tau$, the average chain interpenetration depth theoretically equals the radius of gyration of the whole polymer chain, that is, $d(\tau) \approx R_g$.

Specifically, $d(t)$ for a symmetric polymer interface is given by Zhang and Wool[18] as $d(t) = 0.81R_g$.

Temperature Dependence of Diffusion. The temperature dependence of the diffusion coefficient, D, can be described by the Arrhenius activation energy, the WLF equation, or the Vogel relationship. The Arrhenius activation energy is obtained from the slope of the plot of $\ln D$ vs $1/T$.

$$D = D^* \exp(-E_a/RT) \quad (10)$$

where E_a is the activation energy and D^* is a pressure dependent constant. The quantities R and T represent the gas constant and temperature in degrees Kelvin, respectively.

In another approach, Ferry[23] obtained an apparent activation energy from viscoelastic relaxation data using the WLF equation in the form

$$E_a = 2.303RC_1C_2T^2/(C_2 + T - T_0)^2 \quad (11)$$

where T_0 is a reference temperature (usually T_g) and C_1 and C_2 are quasi universal parameters, dependent on the choice of T_0. When the WLF equation is applied to the temperature dependence of the diffusion coefficient, the corresponding temperature shift factor, a_t, can be represented by[21]

$$\log(a_t) = \log\left[\left(\frac{DT_0}{D_0T}\right)\right] = \frac{C_1(T - T_0)}{C_2 + T - T_0} \quad (12)$$

where D_0 is the diffusion coefficient at the reference temperature, T_0.

In the WLF analysis, the magnitude of E_a depends on the temperature T as described by eq 11. The theory takes into account the fractional free volume change with temperature when the "time scale" of the experiment is long and the temperature is above the T_g. The probability of the barriers, for chain segment rotation, chain cooperative motion, or reptation, is the Arrhenius type and is incorporated in the WLF theory. As a result a relationship is obtained between the "time scale" and inverse absolute temperature of the experiment. At a short "time scale" of measurements or high temperatures the Arrhenius processes are controlling those physical events which are dependent on the fractional free volume, such as viscosity or diffusion. Therefore at long "time scales" or lower temperatures the WLF equation, otherwise the Arrhenius relationship, is expected to give better temperature dependency relationships. The WLF theory predicts a strong temperature dependence for the activation energy, while the Arrhenius relation takes it as a constant for a small temperature interval. Both of these correlations are compared with data from this work and the literature.

The Vogel relation

$$\log(D/T) = A - B/(T - T_\infty)$$

using the coefficients from Wool[20] result in an order of magnitude underestimation of the measured diffusion coefficients.

Strength Development during Interface Healing. During the molding of the sample to full density, it is assumed that the particles are deformed into regular dodecahedrons, similar to those found in latex film formation from aqueous dispersion. For latex films, these surfaces were shown to be flat at the scale of the particle radius. Since the polymer chain R_g is smaller than the particle radius in all cases considered herein, the "flat surface" approximation seems reasonable.

The Prager and Tirrell model[34-36] assumed that mechanical property recovery depends on the total molecular crossing density at the interface. They calculated the crossing density for two cases, namely equilibrium or uniform chain end distributions throughout the bulk, and excess chain ends at the initial interfaces. These two cases yielded a one-half and one-quarter power dependence on time, respectively. The fracture stress dependence on time is intimately connected to the relationship used between crossing density and stress. According to the Griffith theory of fracture, crack initiation occurs when the stored elastic energy equals the energy required for the generation of the new crack surface. The new surface alone accounted for only a tiny fraction of the work required. Then, in a virgin linearly elastic polymer, the energy for the fresh crack surface generation was assumed to be proportional to the crossing density. Since the elastic energy release is related to the square of the applied stress, the fracture stress becomes dependent on the one-half power of the crossing density. This then yields a fracture stress dependence on the power of time of one-fourth and one-eighth. Prager and Tirrell argued, however, that in crack healing, which is analogous to the healing of latex particle interfaces, the stored elastic energy is different from the virgin polymer case. Consideration that at small healing times the stored energy is concentrated in the weakened regions leads to a more reasonable assumption, when

Table 1. Direct Mini-emulsification Recipe of Polystyrene Latexes

ingredients	weight (g)
Oil Phase	
polystyrene	2.0
cyclohexane	20.0
cetyl alcohol	0.256
stearyl alcohol	0.109
Water Phase	
water	100.0
sodium lauryl sulfate	0.435
cetyl alcohol	0.256
stearyl alcohol	0.109

Table 2. Molecular Weight and Particle Size of Polystyrene Latexes

sample	M_n	M_w/M_n	particle radius (Å)[a]
deuterated PS	150 000	1.02	657
	185 000	1.02	672
protonated PS	150 000	1.05	660
	200 000	1.03	680

[a] Determined by SANS.

relating the fracture stress to the crossing density, rather than the crossing density to the one-half power. Thus, Prager and Tirrell predict the fracture stress development with time to be one-fourth power at early times of healing, when chain ends residing on the initial surface cross the interface, which dependence changes over to one-half power later on, when chains from the bulk start to cross the interface.

The Wool model,[18,19] in contrast, is based on the assumption that the fracture stress depends on the interpenetration distance. With the chain end distribution taken as uniform through the bulk, they found that the fracture stress is dependent on time to the one-fourth power.

Experimental Section

Direct Mini-emulsification. In order to prepare latexes having a narrow molecular weight distribution and good particle size uniformity, a direct mini-emulsification technique was used. Anionically polymerized deuterated and protonated polystyrenes having a narrow molecular weight distribution ((DPS) M_n = 150 000 and 185 000, M_w/M_n = 1.02; (HPS) M_n = 200 000, M_w/M_n = 1.03) were obtained from Pressure Chemicals, and M_n = 150 000 protonated polystyrene (M_w/M_n = 1.03) was obtained from Shell Oil Co. as a 6.7 wt % solution in cyclohexane. All experimental conditions employed were identical with those of previous experiments.[16,17] Detailed experimental procedures were described in the previous papers.[16,17] The recipe is shown in Table 1. Polystyrenes were dissolved in cyclohexane with cosurfactants, cetyl alcohol and stearyl alcohol, and then mixed with the water phase containing sodium lauryl sulfate (anionic surfactant) and more cosurfactants. This crude emulsion was homogenized using an ultrasonicator and then filtered through a polycarbonate membrane. This filtration process was used to reduce further the size distribution of the swollen droplets of the polymer solution. Finally, cyclohexane was removed by steam distillation.

Characterization. The particle sizes of the latexes in aqueous dispersion were characterized by photon correlation spectroscopy (Coulter N4MD) and in the dried state by transmission electron microscopy (TEM, Philips 300). A polydispersity index of 1.05 was calculated from electron photomicrography. The latex dispersions were also studied by SANS to obtain a third measure of the particle dimensions. The TEM results show good agreement with SANS data within the experimental error range ±5%. Table 2 shows the collected data for molecular weight and particle sizes of the polystyrene latexes used in the present experiments.

Gel permeation chromatography (Waters) was used to check the possibility of chain breakage during the sonification process. The results indicated that less than 5% chain breakage occurred during formation of the latex.

Table 3. Annealing Conditions of Polystyrene Samples for SANS Measurement

mol wt	annealing temp (°C)	sample name
150 000–150 000 (DPS–HPS)	125	S150125
	135	S150135[a]
	145	S150145
	155	S150155
185 000–200 000 (DPS–HPS)	125	S185125
	135	S185135
	145	S185145[a]
	155	S185155
	165	S185165

[a] These samples have tensile strength data.

Sample Preparation. Pure Latexes. The deuterated and protonated latexes were mixed to give 6 mol % of deuterated polystyrene. The mixed latexes were dried at 50 °C for 2 days, cleaned seven or eight times with excess methanol to remove cosurfactants (cetyl alcohol and stearyl alcohol), extracted in hot distilled water to remove the surfactant (sodium lauryl sulfate), and then dried in a vacuum oven at 60 °C for 5 days. Fourier transform infrared spectroscopy (FT-IR) and differential scanning calorimetry (DSC) showed that substantially all of the surfactants and cosurfactants were removed.

The dried polystyrene particles were pressed by using a computer-controlled hydraulic hot press at 110 °C for 20 min under a pressure of 10 MPa to yield a transparent film of 1.0 mm thickness. Flotation in aqueous NaCl solution gave an average density of 1.055 ± 0.003 g/cm^3 for the blended sample and 1.051 ± 0.004 g/cm^3 for protonated polystyrene (theoretical density = 1.058 and 1.053 g/cm^3, respectively). Thus, the films can be regarded as being fully dense. Since the sintering conditions minimized initial chain interdiffusion between neighboring particles, the sintered films were very brittle.

The polystyrene films were annealed at several different temperatures for various times in sandwich form with a steel spacer between two steel plates in a forced convection oven. Thirty minutes of temperature equilibration was allowed before annealing time was started. The same procedures were employed to prepare 100% protonated specimens for the SANS blank samples and tensile strength test. Annealing conditions of samples are shown in Table 3. The character "S" and the first three numbers designate the "sample" and the molecular weight of deuterated polystyrene, respectively, and the last three numbers define the annealing temperature (°C).

Latexes Containing Cosurfactants. In order to make the latex sample containing cosurfactants, the surfactant (SLS) was first removed. Then, the concentration of cosurfactants was checked by weighing the dried latex after each methanol washing. The concentration of 1.5 wt % obtained after two methanol washes avoids phase separation following the sintering process. The final latex was dried in a vacuum oven at 35 °C for 5 days. Differential scanning calorimetry (DSC) was used to check the glass transition temperature of the polystyrene latex having cosurfactants. The T_g was 100.5 ± 0.5 °C, about 5 deg lower than that of the pure polystyrene latex. The dried polystyrene particles were sintered at 105 °C for 20 min under a pressure of 10 MPa and annealed as above.

The density of all samples was also determined to check the fully dense film and the evaporation of cosurfactants during the course of annealing. The theoretical density of polystyrene containing 1.5 wt % of cetyl alcohol and stearyl alcohol (weight ratio of CA:SA = 7:3) is estimated to be 1.050 g/cm^3. The measured density of the samples (0–90 min annealed samples) gave an average of 1.049 ± 0.003 g/cm^3. There was no measurable change in density with annealing.

SANS Measurements. The SANS experiments were carried out at the National Institute of Standards and Technology, NIST, in Gaithersburg, MD. Disk specimens with 1.0 mm thickness and 1.3 cm diameter were used throughout the measurements. The original size of the deuterated polystyrene latex particles in the dispersed state was measured in a quartz cell having a 2 mm

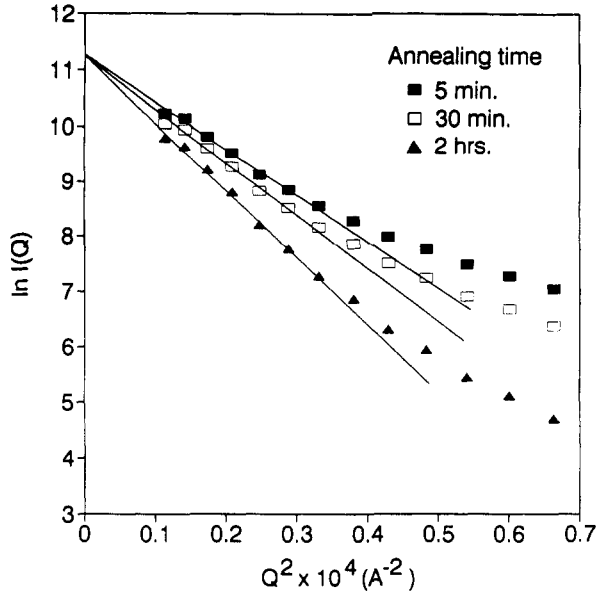

Figure 1. Determination of deuterated polystyrene particles radii of gyration via Guinier plots.

Table 4. Summary of Average Interpenetration Depth (Å) with Annealing Time

	sample			
annealing time	S185125	S185135	S185145[a]	S150135
5 min	18	24	46	36
10 min			54	47
15 min		29	64	
30 min	26	38	113	62
40 min				71
1 h	27	58	159	97
2 h		98	227	136
3.3 h		126		
4 h	46			211

[a] Kim, K. D.; Sperling, L. H.; Klein, A.; Wignall, G. D. *Macromolecules*, in press.

path length. A neutron wavelength of 6.0 Å ($\Delta\lambda/\lambda = 30\%$) was used, with 1.2 cm in diameter sample slits being separated from the source (5 cm × 5 cm) by a distance of 14.77 m. The sample-to-detector distance was 13.18 m. A two-dimensional position sensitive detector (65 × 65 cm² with 1 cm resolution) with a circular pinhole collimation system was employed. With this configuration, SANS data were collected over the range of scattering vectors $0.003 \leq Q \leq 0.034$ Å^{-1}. The recorded intensities for the samples and blanks were radially averaged and converted to absolute values.

Tensile Strength Test. An Instron Universal Testing Machine was utilized to measure the tensile strength of 100% protonated polystyrene samples. Dumbbell-type specimens were prepared by grinding the rectangular films (1 cm × 6 cm) with a fine file, followed by rubbing the ground surface with fine sandpapers until smooth. A grip separation distance of 1.0 cm and a grip separation rate of 0.254 cm/min were applied.

Results

The radii of gyration of the particles were determined by Guinier plots for various annealing times (Figure 1). The average interpenetration depth was calculated by subtracting the radius of the original deuterated latex particles from the radius of the annealed deuterated latex particles; see Table 4. The radius of gyration of the sintered particles is slightly larger than that of the original latex particles due to the nonsphericity of the particles after the high-pressure sintering process. However, 30 min of temperature equilibration was allowed in the present annealing process. During this period, the particle anisotropy is believed to be significantly lost by physical relaxation. Thus, the apparent expansion of the radius of gyration can be observed only after a short period of annealing.

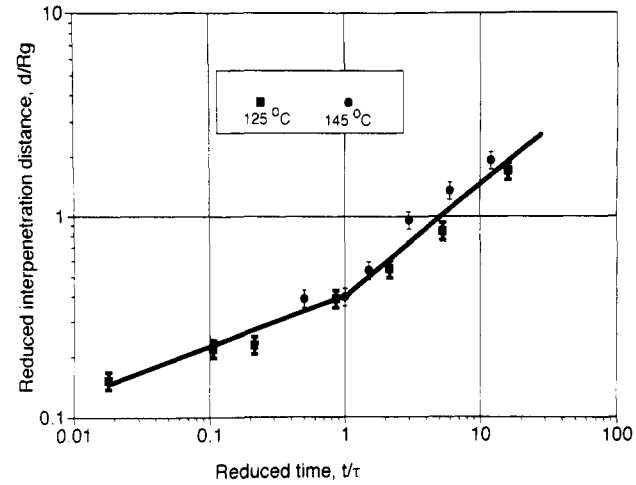

Figure 2. Evaluation of the scaling law time dependence for molecular interdiffusion during annealing of deuterated latex films.

Table 5. Time Dependence of the Average Interpenetration Depth: Slope of the log(depth) – log(time) Plot

		exponent value	
sample	reptation time (τ) (mix)	$t < \tau$	$t > \tau$
S185145	10	0.28 ± 0.02	0.58 ± 0.03
S185135	30	0.26 ± 0.01	0.60 ± 0.02
S185125	281	0.23 ± 0.03	0.51 ± 0.02

To evaluate the scaling law of time dependence, $\log d/R_g$ vs $\log t/\tau$ was plotted in Figure 2. The data approximately followed a $d(t) \propto t^{1/4}$ relationship predicted at short annealing times, which changes over to somewhat higher than the $d(t) \propto t^{1/2}$ predicted at long annealing times; see Table 5. The slope transition break at $t/\tau = 1$ is close to the theoretical reptation time, as predicted by Wool[14] from the minor chain reptation model; however, the d/R_g break should be at $d/R_g = 1$, but is obviously lower. This may be related to the fractal aspects of the problem, discussed below.

From the SANS data, Q-constant and t-constant diffusion coefficients were obtained by using eqs 6 and 7. Figure 3, showing selected data at three different angles (Q = 0.005365, 0.006557, and 0.00749 Å^{-1}), yields the Q-constant diffusion coefficients, D_Q. The time range is from 0 min (just sintered) to 2 h. Surprisingly, all the data points follow the same line, which means that D_Q does not change with scattering angle Q. Anderson and Jou[4] reported that the diffusion coefficient increases with Q. They attributed this apparent Q dependence to instrumental effects, specifically, to the "smearing" of the experimental data. Three factors were mentioned as a cause of this effect: (1) distribution of neutron energies; (2) source–sample–detector geometry; (3) digitization characteristics of the area detector. However, the present Q-constant diffusion coefficients do not show any Q dependence, revealing that the present diffusion data obtained from the decay profile of scattering intensity with annealing time are self-consistent in the experimental Q and time range.

Besides the Q-constant diffusion coefficient, the t-constant diffusion coefficient, D_t, yields interesting information about the dependence of chain motion on diffusion time at polymer interfaces. At annealing times shorter than the reptation time, the chain motion primarily involves moving into a new reptation tube. Since seg-

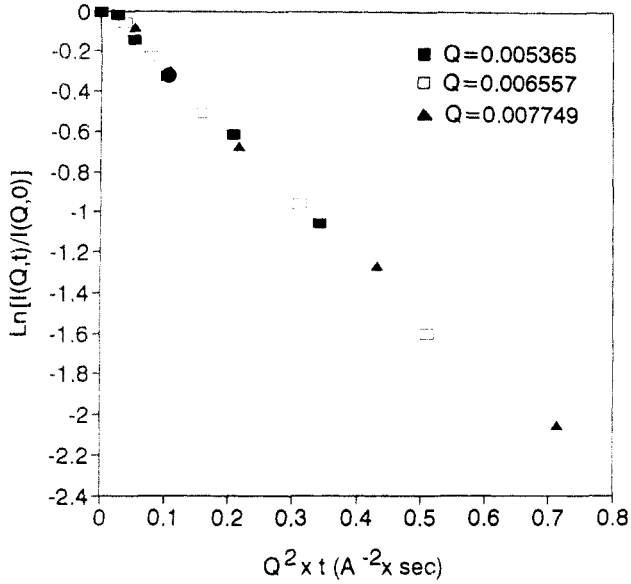

Figure 3. SANS data taken with annealing time for several scattering angles, Q (M_n = 185 000, annealing temperature = 135 °C).

Table 6. Time-Constant Diffusion Coefficient Variation (unit: 10^{-16} cm²/s)

	sample		
annealing time	S150135	S185135	S185125
10 min	1.33		
30 min	1.52	1.56	0.20
40 min	2.25		
1 h	2.75	1.60	0.32
2 h	2.60	1.50	
3.3 h		1.50	
4 h	2.33		0.27
12 h			0.16
24 h			0.17
72 h			0.12

mental motion dominates the diffusion process in this period of time, the diffusion coefficient should be regarded as a segmental diffusion coefficient. Therefore, a real center-of-mass diffusion can be measured only at $t > \tau$. Hahn et al.[1,2] and Winnik et al.[7,8,10,12] observed a decrease of the diffusion coefficient with time during latex film formation. It is reported that this effect is due to the strong molecular weight dependence of D. While short chains dominate diffusion at early diffusion times, longer chains are becoming more prominent at long time, which resulted in the decrease of D with time. However, in the case of uniform chain distribution like in the present system, D is expected to be time independent during film formation.

As seen in Table 6, diffusion data show a constant value after the reptation time as predicted. The Q-constant diffusion coefficients which covered all annealing time range are 2.36×10^{-16}, 1.51×10^{-16}, and 0.16×10^{-16} cm²/s for the sample S150135, S185135, and S185125, respectively. These values are almost the same as the time-constant diffusion coefficients at $t > \tau$. Also, the S150135 and S185135 sample diffusion coefficients show the expected scaling with molecular weight to the −2 power.

The temperature dependence of chain diffusion was evaluated by using the Arrhenius relationship. The t-constant diffusion coefficients of samples annealed at several annealing temperatures for 30 min were obtained from the plot in Figure 4. log D is plotted versus $1/T$ to obtain the activation energy in Figure 5. The activation

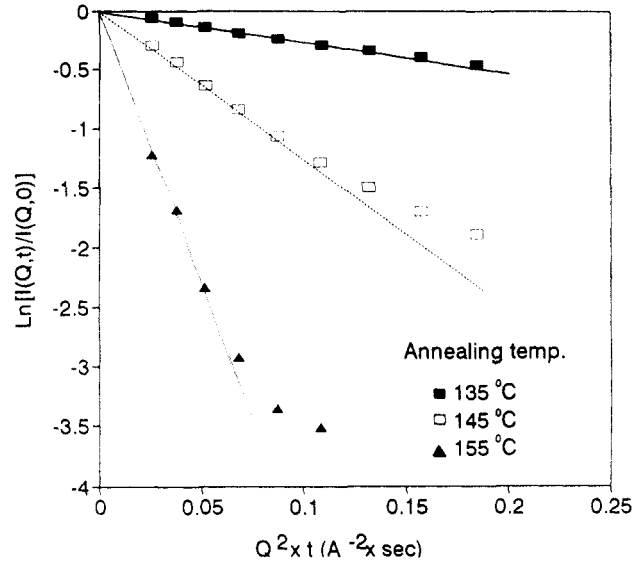

Figure 4. Determination of time-constant diffusion coefficients from SANS data (M_n = 185 000, annealing time = 30 min).

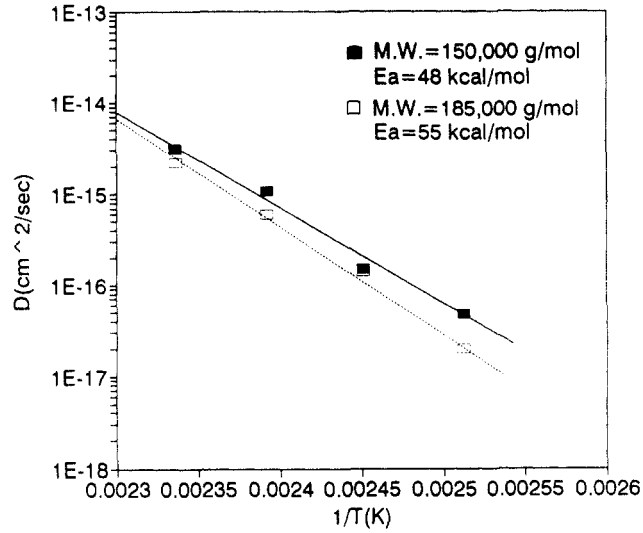

Figure 5. Arrhenius plots (log D vs $1/T$) to calculate the activation energy.

Table 7. Selected Diffusive Activation Energies (E_a) of Polystyrene from Arrhenius Plots

mol wt	temp (°C)	E_a (kcal/mol)	ref
199 000	125–146	64	17
43 700	170–180	40	22
2 400	180	15	23
185 000	125–155	55	*a*
150 000	125–155	48	*a*

[a] Present work.

energies, E_a, were 52 ± 4 kcal/mol for the molecular weights of 185 000 and 150 000. The current activation energy is compared with literature results in Table 7, showing a good agreement with E_a obtained by others. It is also interesting to relate the activation energy from diffusion coefficients with that obtained by the measurement of dynamical mechanical properties. As described in the theory section, an apparent activation energy from viscoelastic relaxation can be calculated by eq 11. By using parameters obtained by Barlow et al.,[39] C_1 = 13.7 and C_2 = 50, and T_0 = 100 °C as a reference temperature, E_a was calculated as 56–80 kcal/mol in the experimental temperature range $130 \le T \le 150$ °C. This result matches the value obtained from Figure 5.

Table 8. Summary of SANS and Tensile Strength Test Results of Polystyrene Latex Films (M_n = 150 000, annealing temperature = 135 °C)

annealing time	R_g (Å)	radius (Å)	av depth of penetration (Å)	tensile strength (10^5 N/m^2)
latex	509	657		
sintered	544	702		103
5 min	537	693	36	145
10 min	545	704	47	175
30 min	557	719	62	246
40 min	564	728	71	266
1 h	584	754	97	315
2 h	614	793	136	273
4 h	672	868	211	312

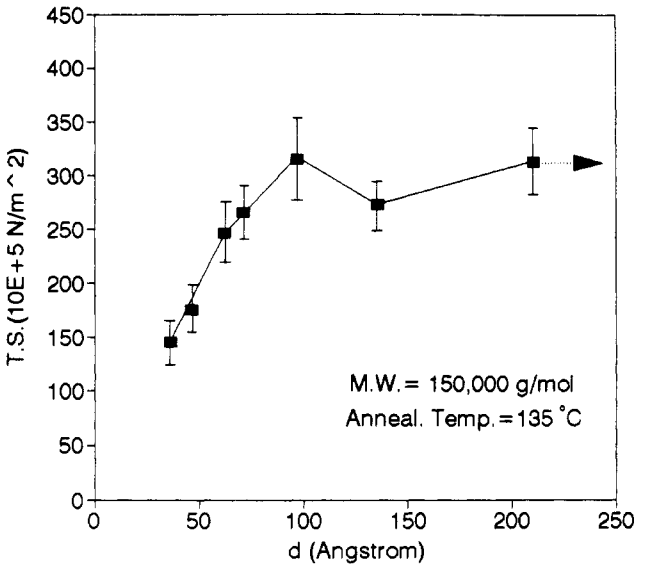

Figure 6. Tensile strength first increasing, going through a maximum, and then decreasing. It increases again and finally shows a plateau value.

Table 8 and Figure 6 represent the tensile strength buildup feature as a function of the average interpenetration depth. It is noted that the present system shows a maximum tensile strength at an average interpenetration depth of about 90–100 Å. Zhang and Wool[18] predicted that the maximum fracture energy occurs at the interpenetration depth of X, given by $X_\infty = 0.81R_g$, which predicts a value of 86 Å for a molecular weight of 150 000. However, this tensile strength was fully developed only at much longer annealing times than the theoretical reptation time. It was also observed in the previous study[17] and will be discussed later. In addition, it is observed that tensile strength shows a maximum value, drops, and then recovers to a constant value. This unusual feature was also observed in a study of the fracture energy and chain scission of latex films by Mohammadi et al.[41,42] It is attributed to a change in the fracture path from along the latex interfaces to straight through the material.

In Figure 7, the diffusion rates between pure latex and latex containing the cosurfactants are compared. The annealing temperatures of both systems were 30 deg higher than T_g, which were 130 °C for the polystyrene latex with cosurfactants and 135 °C for the pure polystyrene latex, respectively. Interestingly, data from both systems do not show a big difference up to the reptation time. However, after the reptation time, polystyrene chains having cosurfactants interdiffuse faster than the pure chains. This may indicate that cosurfactants do not significantly affect the diffusion rate when segmental motion dominates the diffusion process. However, when

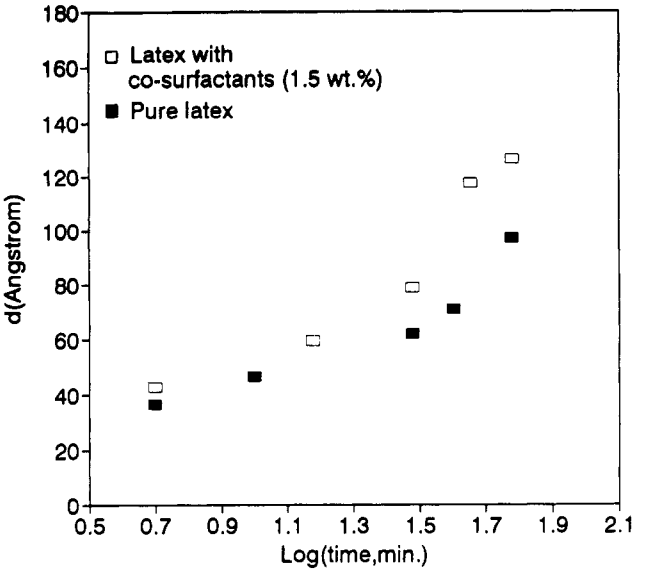

Figure 7. Plot of interpenetration depth vs annealing time during film formation from latex with cosurfactants compared with that obtained by Kim et al.

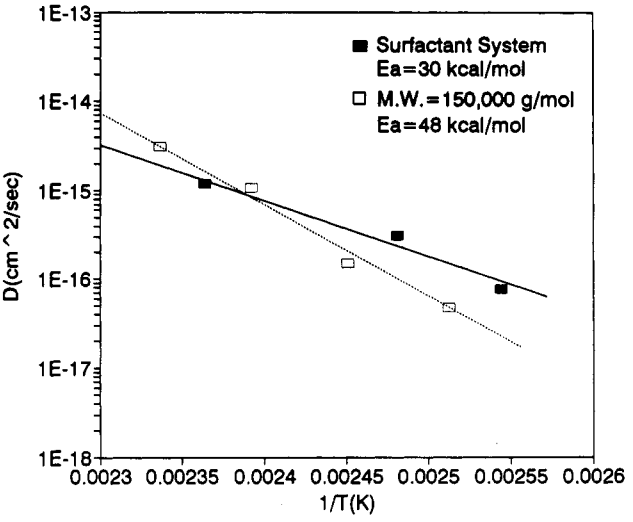

Figure 8. Arrhenius plots (log D vs $1/T$) to calculate the activation energy from diffusion data of latex containing cosurfactants compared with that obtained by Kim et al.

the chains move randomly at $t > \tau$, there is an increase in the polymer diffusion rate by the presence of small amounts of cosurfactants. This may be due to the plasticizing effect of the cosurfactants which increases the free volume between chains.

In order to evaluate this effect in another way, the activation energies were also compared. Figure 8 illustrates a plot of log D vs $1/T$ to obtain the activation energy from the slope. For polystyrene with cosurfactant the activation energy is 30 kcal/mol in the experimental temperature range $120 \leq T \leq 140$ °C, a considerably smaller value than that of the pure polystyrene latex, E_a = 48 kcal/mol.

Discussion

***Q* Dependence of the Radius of Gyration.** The calculation of the radius of gyration from the Guinier plot must satisfy the Guinier criterion, $Q^2R_g^2 < 1$. In the present system, in order to observe the Guinier region the radius of gyration should be smaller than 300 Å in the range $0.003 \leq Q \leq 0.001$ Å^{-1} for λ = 6 Å. Another way to satisfy this condition is to increase the wavelength, λ, which results in a reduction of the Q values because Q is equal to $(4\pi/\lambda)\sin(\theta/2)$. However, since the scattering intensity is

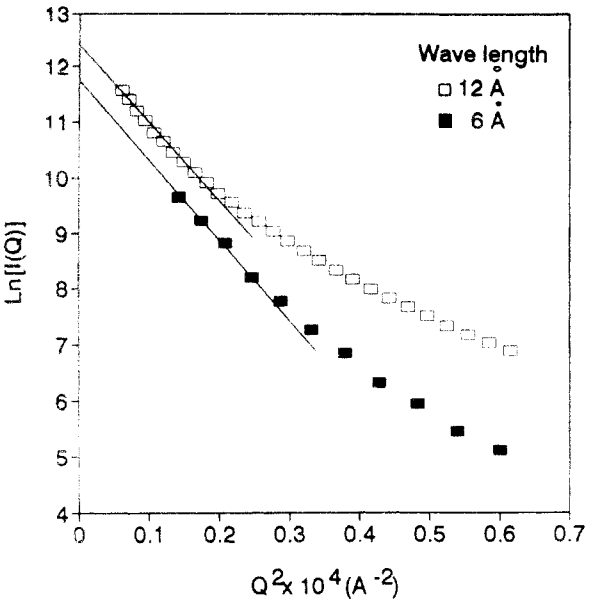

Figure 9. Comparison of Guinier plots for two different wavelengths (λ = 6 and 12 Å).

inversely proportional to the fourth power of λ, there is an increase in the time needed to run an experiment. In the current study, the neutron wavelength was fixed at λ = 6 Å during the SANS measurements. For comparison purposes, one series was measured at two different wavelengths, that is, λ = 6 and 12 Å, Figure 9. The upper plot (λ = 12 Å), having several data points in the Guinier region, shows practically the same slope as the lower plot (λ = 6 Å). As a consequence, it can be said that the radius of gyration values calculated at λ = 6 Å are reasonably reliable in spite of the relatively few points that lie in the Guinier Region.

Time Dependence of Tensile Strength Development. Latex film formation can be considered as a special case of interface healing, such as crack healing and polymer welding. In both cases, strength development is dependent upon polymer chain interdiffusion. Generally, an interface gains strength with healing time to the one-fourth power in the crack healing of linear random coil systems such as poly(methyl methacrylate) and polystyrene.[37,38] The tensile strength buildup during latex film formation was investigated by Yoo et al.,[5,6] also showing a one-fourth power time dependence.

To evaluate the time dependence of tensile strength buildup, the experimental points were plotted on a log–log scale in Figure 10. The reptation time of this system is 24 min. A straight line has a slope of 0.62 ± 0.05. This result can be interpreted as follows.

As predicted by Prager and Tirrell[34–36] in the chain-crossing density model, chain end location plays an important role in developing mechanical strength, especially at short annealing times. In general, a fresh crack surface contains many chain ends as a result of scission during the fracture. However, since the anionic polymerized polystyrene has a nonpolar hydrogen end group, it can be assumed that chain ends are uniformly distributed through the latex particles in the present direct mini-emulsification system. In that case, tensile strength development should follow a $t^{1/2}$ behavior, corresponding to a healing process where chain ends are randomly located in the particle at the early stage.

Wool et al.[14,18] introduced another property of the interface, namely, the number of chain segments crossing the interface, $N(t)$. Theoretically, $N(t)$ shows a $t^{3/4}$

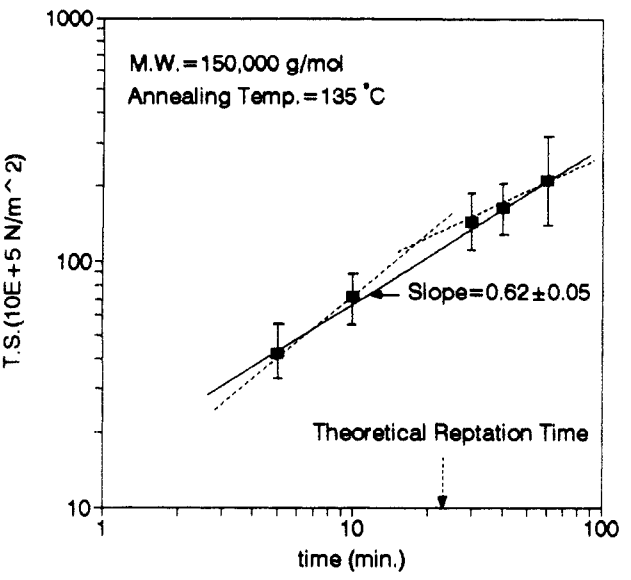

Figure 10. log–log plot showing the increase in tensile strength with annealing time.

Table 9. Comparison of Self-Diffusion Coefficients of Polystyrene Measured by SANS with Other Techniques

M_n	temp (°C)	D (cm²/s)	D^a (cm²/s)	analytical method	ref
96 000	212	1.6×10^{-11}	6.6×10^{-12}	Raleigh scattering	43
233 000	120	5.5×10^{-18}	1.3×10^{-17}	FRS	44
199 000	136	1.7×10^{-15}	2.0×10^{-15}	IMS	20
115 000	160	8.1×10^{-14}	4.8×10^{-14}	SANS	45, 46
68 000	130	1.8×10^{-15}	3.7×10^{-16}	SANS	4
150 000	135	2.4×10^{-16}	2.4×10^{-16}	SANS	*b*

[a] Converted to the same molecular weight (M_n = 150 000) by using $D \propto M^{-2}$. [b] Present work.

dependence up to the reptation time due to correlated motion effects, reverting to a $t^{1/2}$ dependence at $t > \tau$. The present slope of 0.62 ± 0.05 lies between 0.5 and 0.75, because the reptation time lies near the middle of the data shown in Figure 10.

Temperature Dependence of *D*. In Figure 5, the activation energies for molecular diffusion were obtained by using a temperature independent Arrhenius equation (eq 10). However several studies[4,20,22] showed that E_a increases with decreasing experimental temperature. As T_g is approached, the polymeric chain loses its mobility, and E_a approaches large values at $T = T_g$. Some published self-diffusion coefficients of polystyrene including the present results are summarized in Table 9. All data were converted to the same molecular weight, M_n = 150 000, using the relationship, $D \propto M^{-2}$. These reduced D values are plotted with the diffusion temperature to calculate the activation energy in Figure 11. The activation energy was 65 ± 5 kcal/mol, which is bigger than that (48 kcal/mol) from the present SANS data. This is probably due to the error in the Arrhenius relationship as T_g is approached.

Chain End Group Distribution Effect on the Diffusion. Although most diffusion studies using bulk polymers have followed the existing theories[14,15,28,32,36] in this area, the present latex system shows some differences from the corresponding bulk systems.

Wool[18] predicted that chains attain equilibrium entanglements when $t = \tau$ and $d(t) \simeq R_g$ and show a plateau mechanical strength when $d(t)$ equals $0.81R_g$, assuming a symmetric interface.

As seen in Figure 2, the average interpenetration depth at $t = \tau$ is about 40–50 Å, comparable to half the radius

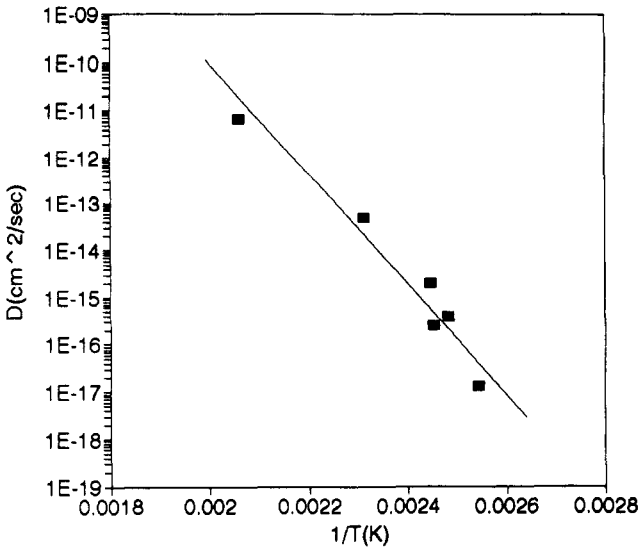

Figure 11. Arrhenius plot to see the relationship among published diffusion data at several diffusion temperatures. All data are from Table 9.

of gyration of the whole polystyrene chain. This interpenetration distance value may be grossly underestimated. This is due to the assumptions used in calculating the radius of the expanding deuterated particle from the radius of gyration measured from SANS. The smooth sphere approximation must be in error since in the later stages of molecular interpenetration, close to R_g and beyond, the expanding sphere is more like the shape of a starburst. This was clearly shown in our earlier work, when from a Porod power law plot the smooth spherical starting surface was found to change over to a mass fractal as the interdiffusion process proceeded.[17] SANS measurement provide a model independent R_g value, but in the present calculations a hard sphere model was assumed to calculate the radius. For the same R_g, but for a mass fractal, the radius of interpenetration is larger. In a subsequent note the fractal treatment will be shown to explain in part the discrepancy illustrated in Figure 2. However, in Figure 6, tensile strength was fully developed at an interpenetration depth comparable to the $0.81R_g$, agreeing with theory without fractal corrections. With fractal corrections full tensile strength is developed at an interpenetrating distance larger than R_g. This is not consistent with Wool's prediction of $d(t) = 0.81R_g$ (86 Å). A third point is that annealing times for full tensile strength were longer than the theoretical reptation time, apparently contradicting theory. Overall, the agreement with the Wool theory is fair, especially noting possible experimental errors. A similar result was observed in the previous study.[17]

In the present direct mini-emulsification system, it is assumed that chain ends are randomly distributed through the latex particles due to the nonpolar hydrogen end group. These chain ends inside latex particles need to diffuse for longer times before they can contribute to interparticle entanglement formation, depending on the distance of the chain ends from the surface.

Conclusions

The polymer diffusion process during latex film formation was studied by SANS. An improved direct mini-emulsification technique was used to prepare artificial latexes. The chain interpenetration depth and diffusion coefficients were obtained from SANS data around the reptation time, and the activation energy was calculated by the Arrhenius equation.

The average chain interpenetration depth was dependent on the one-fourth power of the annealing time up to the reptation time. This was shifted to the one-half power after the reptation time, as predicted by Wool. Diffusion data represent the center of mass diffusion at annealing times longer than the reptation time. The present diffusion coefficients are of the same order of magnitude as those of bulk and planar geometry samples. However, the latex film formation system shows an interdiffusion distance at a certain annealing time shorter than that in the bulk system due to the specific sample geometry.

Diffusive activation energies of 52 ± 4 kcal/mol were obtained for molecular weights of 185 000 and 150 000, respectively, in the temperature range $125 \leq T \leq 155$ °C, comparable to the activation energy obtained from dynamic mechanical measurements.

The tensile strength was fully developed at a penetration depth comparable to 0.81 times the weight average radius of gyration of the whole polystyrene chain, as predicted by Wool. However, the diffusion time to reach the maximum tensile strength is longer than the theoretical reptation time. Tensile strength development showed a 0.62 ± 0.05 power time dependence. Finally, the effect of cosurfactants (cetyl alcohol and stearyl alcohol) on the diffusion rate as a plasticizer was investigated during the latex film formation. Interestingly, the polymer diffusion rate was affected only at times longer than the reptation time by a small amount of cosurfactants. The activation energy (30 kcal/mol) from the Arrhenius plot showed a value lower than that (48 kcal/mol) of the pure polystyrene latex.

Disclaimer

Certain equipment and instruments or materials are identified in this paper in order to adequately specify the experimental conditions. Such identification does not imply recommendation by the National Institute of Standards and Technology nor does it imply that the materials are necessary the best available for the purpose.

Acknowledgment. The authors wish to thank the Emulsion Polymer Institute and the Polymer Interfaces Center in Lehigh University for support. The SANS experiments were performed at the CHRNS 30-m SANS instrument in the National Institute of Standards and Technology (NIST). We acknowledge the support of NIST, U.S. Department of Commerce, in providing the facilities used in this experiment. This material is based upon activities supported by the National Science Foundation under Agreement No. DMR-9122444 and CTS-8820705.

References and Notes

(1) Hahn, K.; Ley, G.; Schuller, H.; Oberthur, R. *Colloid Polym. Sci.* **1986**, *264*, 1092.
(2) Hahn, K.; Ley, G.; Oberthur, R. *Colloid Polym. Sci.* **1988**, *266*, 631.
(3) Linne, M. A.; Klein, A.; Miller, G. A.; Sperling, L. H.; Wignall, G. D. *J. Macromol. Sci., Phys.* **1988**, *B27* (2 & 3), 217.
(4) (a) Anderson, J. E.; Jou, J. H. *Macromolecules* **1987**, *20*, 1544. (b) Jou, J. H. Ph.D. Dissertation, The University of Michigan, 1986.
(5) Yoo, J. N.; Sperling, L. H.; Glinka, C. J.; Klein, A. *Macromolecules* **1990**, *23*, 3962.
(6) Yoo, J. N.; Sperling, L. H.; Glinka, C. J.; Klein, A. *Macromolecules* **1991**, *24*, 2868.
(7) Pekcan, O.; Winnik, M. A.; Croucher, M. D. *Macromolecules* **1990**, *23*, 2673.
(8) Zhao, C. L.; Wang, Y.; Hruska, H.; Winnik, M. A. *Macromolecules* **1990**, *23*, 4082.
(9) Wang, Y.; Winnik, M. A. *Macromolecules* **1990**, *23*, 4731.

(10) Wang, Y.; Zhao, C. L.; Winnik, M. A. *J. Chem. Phys.* **1991**, *95*, 2143.
(11) Winnik, M. A.; Wang, Y.; Haley, F. *J. Coat. Technol.* **1992**, *64*, 51.
(12) Wang, Y.; Winnik, M. A. *J. Phys. Chem.* **1993**, *97*, 2507.
(13) Wool, R. P.; O'Connor, K. M. *J. Appl. Phys.* **1981**, *52*, 5194.
(14) Kim, Y. H.; Wool, R. P. *Macromolecules* **1983**, *16*, 1115.
(15) de Gennes, P. G. *J. Chem. Phys.* **1971**, *55*, 572.
(16) Mohammadi, N.; Kim, K. D.; Klein, A.; Sperling, L. H. *J. Colloid Interface Sci.* **1993**, *157*, 124.
(17) Kim, K. D.; Sperling, L. H.; Klein, A.; Wignall, G. D. *Macromolecules*, in press.
(18) Zhang, H.; Wool, R. P. *Macromolecules* **1989**, *22*, 3018.
(19) Wool, R. P.; Yuan, B. L.; McGarel, O. *J. Polym. Eng. Sci.* **1989**, *29*, 1341.
(20) Whitlow, S. J.; Wool, R. P. *Macromolecules* **1991**, *24*, 5926.
(21) Nemoto, N.; Landry, M. R.; Noh, I.; Yu, H. *Polym. Commun.* **1984**, *25*, 151.
(22) Antonietti, M.; Coutandin, J.; Grutter, R.; Sillescu, H. *Macromolecules* **1984**, *17*, 798.
(23) Bachus, R.; Kimmich, R. *Polymer* **1983**, *24*, 964.
(24) Antonietti, M.; Coutandin, J.; Sillescu, H. *Makromol. Chem., Rapid Commun.* **1984**, *5*, 525.
(25) Voyutskii, S. S. *J. Polym. Sci.* **1958**, *32*, 528.
(26) Zhao, C. L.; Holl, Y.; Pith, T.; Lambla, M. *Colloid Polym. Sci.* **1987**, *265*, 823.
(27) Urban, M. W.; Evanson, K. W. *Polym. Commun.* **1990**, *31*, 279.
(28) Ferry, J. D. *Viscoelastic Properties of Polymers*, 3rd ed.; Wiley: New York, 1980.
(29) Guinier, A.; Fournet, G. *Small Angle Scattering of X-rays*; John Wiley and Sons: New York, 1955.
(30) Summerfield, G. C.; Ullman, R. *Macromolecules* **1987**, *20*, 401.
(31) Summerfield, G. C.; Ullman, R. *Macromolecules* **1988**, *21*, 2643.
(32) de Gennes, P. G. *Macromolecules* **1976**, *4*, 587.
(33) Doi, M.; Edwards, S. F. *J. Chem. Soc., Faraday Trans. 2* **1978**, *74*, 1802.
(34) Prager, S.; Tirrell, M. *J. Chem. Phys.* **1981**, *75*, 5194.
(35) Prager, S.; Adolf, D.; Tirrell, M. *J. Chem. Phys.* **1983**, *78*, 7015.
(36) Prager, S.; Adolf, D.; Tirrell, M. *J. Chem. Phys.* **1986**, *84*, 5152.
(37) Kausch, H. H.; Petrovska, D.; Landel, R. F.; Monnerie, L. *Polym. Eng. Sci.* **1987**, *27*, 149.
(38) Kline, D. B.; Wool, R. P. *Polym. Eng. Sci.* **1988**, *28*, 52.
(39) Barlow, A. J.; Erginsay, A.; Lamb, J. *Proc. R. Soc.* **1967**, *A298*, 481.
(40) Roland, C. M.; Bohm, G. G. A. *Macromolecules* **1985**, *18*, 1310.
(41) Mohammadi, N.; Yoo, J. N.; Klein, A.; Sperling, L. H. *J. Polym. Sci., Polym. Phys. Ed.* **1992**, *30*, 1311.
(42) Mohammadi, N.; Klein, A.; Sperling, L. H. *Macromolecules* **1993**, *26*, 1019.
(43) Antonietti, M.; Countandin, J.; Sillescu, H. *Macromolecules* **1986**, *19*, 793.
(44) Green, P. F.; Kramer, E. J. *J. Mater. Res.* **1986**, *1*, 201.
(45) Stamm, M. *J. Appl. Crystallogr.* **1991**, *24*, 651.
(46) Brautmeier, D.; Stamm, M.; Linder, P. *J. Appl. Crystallogr.* **1991**, *24*, 665.